Energy and Buildings 141 (2017) 1–15

Contents lists available at ScienceDirect

Energy and Buildings

journal homepage: www.elsevier.com/locate/enbuild

Impacts of building envelope design factors upon energy loads and their optimization in US standard climate zones using experimental design

Seok-Gil Yong[a,1], Jong-Hyun Kim[a,1], Yuseong Gim[a], Jinho Kim[b], Jinkyun Cho[c], Hiki Hong[a], Young-Jin Baik[d], Junemo Koo[a,*]

[a] Department of Mechanical Engineering, Kyung Hee University, Yongin 446-701, South Korea
[b] Department of Building Technology, Suwon Science College, Hwasung, 445-742, South Korea
[c] Constuction & Energy Business Division, Korea Conformity Laboratories, Jincheon-gun, Chungbuk 27872, South Korea
[d] Thermal Energy Conversion Laboratory, Energy Efficiency Research Division, Korea Institute of Energy Research, Daejeon 34129, South Korea

ARTICLE INFO

Article history:
Received 3 October 2016
Received in revised form 12 February 2017
Accepted 13 February 2017
Available online 15 February 2017

Keywords:
Building energy loads
Building envelope
Design parameters
Optimization
Experimental design
Climate zone

ABSTRACT

The impacts of building envelope design factors upon cooling and heating loads in US cities of different climate zones were quantitatively analyzed using a fractional factorial experimental design. This analysis yielded regression models of the energy loads as functions of the factors considered. The relative importance of building envelope design factors for an office building was statistically compared. The design factors were classified into three groups: (1) a factor directly affected by insolation, SHGC; (2) another group affecting heat transmission based upon the temperature difference between the indoors and the outdoors, WDI, WI, and ACR; and (3) another group affecting the effective area for heat transfer, WWR, AR, FA, CH, and PH. Unique phenomena in different climate zones were further investigated considering the weather features in those zones. Pareto-front curves of cooling and heating loads were obtained, yielding information on optimal design factor sets in the different climate zones. The reasons for the variation in optimal sets of design factors along the Pareto fronts are explicitly explained in terms of the main effects and interaction effects of the design factors.

1. Introduction

Recently, the United States Energy Department announced a large investment to improve the nation's buildings, with the goal of saving the money of American consumers, reducing emissions, and creating new jobs [1]. In the announcement, they stressed the importance of the projects by discussing the significant share of building-related energy consumption in the US and the benefits to the American people and society from the newly funded technologies. The newly funded technologies are composed of four broad technology areas: sensors and controls, HVAC&R and joining technologies, windows and building envelope, and energy modeling. They reported that the high energy demands from commercial buildings could substantially increase the burden on power grids during peak periods and that energy-efficient buildings are the solution for the steady and affordable supply of electricity. The Office of Energy Efficiency & Renewable Energy has introduced Zero Energy Buildings (ZEB), with the two steps of efficient building design and renewable energy supply to accomplish the goal of zero energy consumption. To improve building energy efficiency, Cho et al. [2] reported that passive building design factors should be optimized to minimize building energy loads and that the efficiencies of active components like cooling and heating systems should be enhanced to reduce energy consumption. They claimed that it is cost-effective to consider these factors in the building planning phase.

1.1. Literature review

Various previous reports have addressed the selection of building passive factors to minimize building energy loads under different climate conditions. Caldas and Norford [3] introduced the use of genetic algorithms (GAs) to search for optimal placements and sizes of windows in an office building considering the

* Corresponding author.
E-mail addresses: dydtjrrlf@khu.ac.kr (S.-G. Yong), hyuns16@naver.com (J.-H. Kim), jmkoo@khu.ac.kr (J. Koo).
[1] Co-first authors.

http://dx.doi.org/10.1016/j.enbuild.2017.02.032
0378-7788/

lighting and thermal energy consumption, with the aid of thermal analysis tool DOE2.1E. They stressed that the multiple alternative solutions generated by GAs help designers to determine a solution considering other constraints. Wright et al. [4] performed an optimization of building energy cost and occupant thermal comfort using multi-objective GAs. They concluded that multicriterion genetic algorithm search methods showed potential for identifying trade-offs between the elements of building thermal design. Wetter and Wright [5] compared a set of optimization techniques to solve building design optimization problems based upon discontinuous cost functions. They reported that optimizers requiring smoothness in the cost functions could fail to yield good solutions. Yang et al. [6] compared the energy performance of existing office envelopes in five different climate conditions in China using the overall thermal transfer value (OTTV) method. They compared the results with the corresponding local design codes and suggested that controlling the area-weighted overall heat transfer coefficient under the local design codes is the key to enhancing performance. Jaffal et al. [7] adopted the design of experiments (DOE), also known as experimental design, to find optimal selections of building envelope parameter values for a family house to minimize the heating load. They performed dynamic building energy simulation using TRNSYS and used the linear model obtained from the regression analysis to simulate the outcomes of the designed set of treatments. They applied the developed method to cities in three different climate conditions: continental, oceanic, and Mediterranean. Magnier and Haghighat [8] developed a simulation-based artificial neural network to mimic building responses and used this to perform an optimization of thermal comfort and building energy consumption considering HVAC system settings, thermostat programming, and passive envelope design factors. They reported that both thermal comfort and energy performance could be improved as a result of the optimization. Gong et al. [9] used orthogonal experimental design and one-factor-at-a-time (OFAT) analysis to minimize the total energy consumption of a residential building by selecting the optimal set of seven passive building design factors in 25 different cities in China. They provided a guideline for the optimal selection of the level of each parameter in various Chinese climate zones. Machairas et al. [10] and Nguyen et al. [11] published review articles on the research developments in the use of optimization techniques for building design separately. They summarized the optimization algorithms, tools, and building performance evaluation tools, as well as the optimization targets and objective functions. Schnieders et al. [12] compared the residential Passive Houses in different climate zones all around the world, and they discussed the regional dependence to realize them by performing dynamic building energy simulations. Recently, Delgarm et al. [13] performed an optimization study based on EnergyPlus simulations under four different Iranian climate conditions, taking the annual lighting and cooling energies as the objective functions and the building orientation, window size, and overhang specification as the design factors. They concluded that the optimization of building design factors could significantly lower building energy consumption. Goia [14] reported the optimization research to search for the optimal window-to-wall ratio values in office buildings in different European climates for energy saving by performing EnergyPlus-based thermal and lighting simulations and concluded that the optimum values are found in a relatively narrow range. Xu et al. [15] developed building dynamics regression models using DOE analysis of TRNSYS simulation results. They also performed an optimization study on the cooling and heating loads of an office building using the non-dominated sorting GA to obtain Pareto-front curves representing the optimal building design factor sets that minimize building energy loads. Many researchers have developed building design optimization method for building energy conservation and reported their application to buildings in different locations. However, it was hard to find a study that analyzed the impact of specific climate factors on energy use and the physical meaning of the design alternatives obtained from the optimization process.

In this study, the works of Xu et al. [15] has been expanded by investigating the impacts of climate conditions upon the optimal building design factor sets to minimize the cooling and heating loads of an office building. The causes of the inflection points in Pareto front lines was elucidated in terms of the impacts of the main effects and interaction effects of building design factors.

2. Theory

2.1. Baseline model selection and main assumptions

The same baseline model as that used in Xu et al. [15] was used in this study, with the added consideration of ventilation load according to the guideline in ANSI/ASHRAE Standard 62-2007 [16]. The impacts of altering building design factors upon building heating and cooling loads in different US climate zones were analyzed for a representative floor of a reference building having an exterior core. The reference floor was selected as an office floor since most of an office building is used for this purpose, and the reference building was assumed to be a collection of multiples of this office floor. Due to the limitations of the number of design factors allowed and the difficulty in setting the levels of design factors in the DOE, common design factors considered in previous studies were selected for the current study: floor area (FA), building orientation (OR), ceiling height (CH), aspect ratio (AR), plenum height (PH), window-to-wall ratio (WWR), wall insulation (WI), window insulation (WDI), solar heat gain coefficient (SHGC), and air leakage (ACR). The purpose of this study is to present an overall analysis methodology, and it is not intended to analyze the impact of all architectural design elements on building energy loads. Although the shading, or overhang, could affect the loads seriously, it was not considered in the current study due to the difficulty of handling it as an example [15].

The layouts of 178 buildings in Korea were inspected together with researchers and architects in commercial companies, and it was analyzed that the buildings had about 20–40 stories and 70,000 m^2 of total floor area in average, and 1400 m^2 of average floor area. For the recently built office buildings, the total floor area tends to increase to between 40,000 and 100,000 m^2. The building core usually spans about 25–30% of total floor area, and its location can affect the window area ratio to vary building heating and cooling loads. From the review, the design factors of impact to building heating and cooling loads were selected. Table 1 lists the specifications of the reference building, and Table 2 lists the considered building design factors and their levels of alteration in the DOE. The reference levels of the building design factors were selected to comply with the latest Korean national standard and government guideline. Regarding WWR, there is a Korean government guideline for the design of energy-efficient buildings [17] not to exceed 60%. Considering the area of the exposed core wall, the upper level of WWR was assigned as 52%. The schedules for occupancy, heating/cooling, and lighting were set according to the ASHRAE 90.1-2004 standard. For the equipment schedule, which is not provided in the ASHRAE 90.1-2004 standard, an hourly operation schedule for a large office in the commercial reference building models of national building stock [18] was used. Miami, Phoenix, San Francisco, Baltimore, Chicago, Helena, Duluth, and Fairbanks were selected as representative cities of US climate zones 1–8, respectively [18,19]. Table 3 lists the classifications and features of each zone, as well as the weather file names of TMY2 format provided by the National Renewable Energy Laboratory. The floor consisted of four adjacent thermal zones (Offices 1–4), an air-

Table 1
Summary of reference building.

Category	Subcategory	Value	Reference
Use		Office	
Size	Floor area (m^2)	1444	
	Air-conditioned area (m^2)	1019	
	Floor height (m)	3.9	[18]
	Ceiling height (m)	2.7	[18]
	Window-to-wall ratio (%)	40	[26]
Wall U-value	External wall (W/m^2 K)	0.365	[27]
Window	U-value (W/m^2 K)	2.84	[27]
	SHGC	0.4	[27]
Tightness	Infiltration (ACH)	0.3	[28]
Internal heat gain	People (people/m^2)	0.1	[29]
	Lighting (W/m^2)	12	[27]
	Equipment (W/m^2)	16	[28]
Set temperature	Heating (°C)	20	[30]
	Cooling (°C)	26	[30]
Set humidity	Relative humidity (%)	50	[31]
Outdoor air	Ventilation (L/s/person)	8.5	[32]
Schedule	People		[33]
	Heating/cooling		[33]
	Lighting		[33]
	Equipment		[18]

Table 2
List of factors and their simulated levels.

Factor	Symbol	Level	
		Low (−1)	High (+1)
Floor area (m^2)	FA	1000	2000
Aspect ratio	AR	1	2
Orientation	OR	South	West
Window-to-wall ratio (%)	WWR	25	52 [26]
Ceiling height (m)	CH	2.4	2.9
Plenum height (m)	PH	0.8	1.2
Wall insulation (W/m^2 K)	WI	0.150	0.36 [27]
Window insulation (W/m^2 K)	WDI	0.75	2.84
SHGC	SHGC	0.2	0.7
Air leakage (ACH)	ACR	0.1	0.3 [28]

conditioned core zone, and a plenum space over these as shown in Fig. 1.

The main assumptions of this study are as following:

- Each thermal zone is assumed to be well mixed, and the zone temperature is uniform.
- The thermal zones are separated by massless walls, and the heat transfer coefficient on each side of walls is assumed to be constant 8 W/m^2K.
- The heat transfer coefficients of external walls are assumed to be constants, 8 W/m^2K inside and 18 W/m^2K outside.
- There is no shading effect from other buildings.
- The weather data in the TMY2 format of selective cities in the US were used in the simulation.

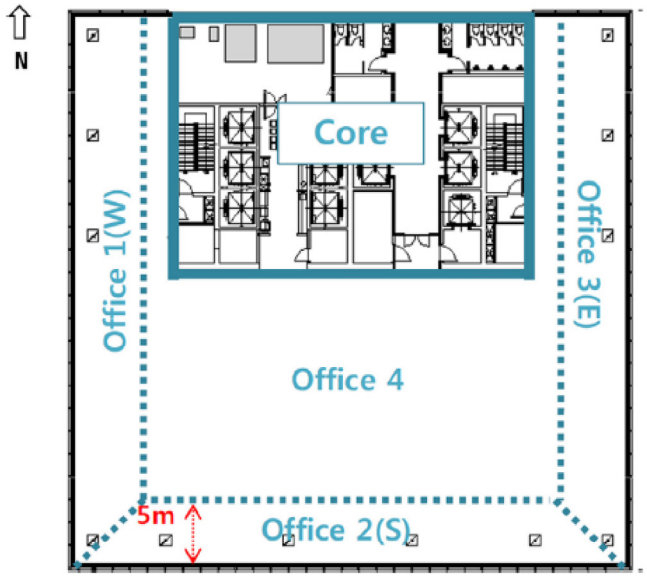

Fig. 1. Floor layout of the reference building [15].

- The operation parameters affecting indoor conditions, thermal transmissions, and internal heat gains are summarized in Table 1.

Although the results and conclusions drawn from this study are limited to the cases under the given assumptions, they could be taken as a typical example case of applying the developed analysis methodology. To extend the developed method for the general use, it is necessary to adjust the number of design factors considered and their lower & upper levels for the given problem.

2.2. Experimental design

As introduced by Xu et al. [15], experimental design or design of experiments is composed of analysis of variance (ANOVA), regression, and optimization processes. It can be used systematically to analyze the functional dependence of the building cooling and heating loads upon the building envelope design factors of FA, OR, CH, AR, PH, WWR, WI, WDI, SHGC, and ACR.

The sum of the main effects of factors and the second-order interaction effects between pairs of factors comprises the functional relation between the factors and the outputs. Higher-order interaction terms could be confounded by the remaining main and interaction effects using the experimental design principles of confounding and orthogonality, thereby reducing the number of runs required to analyze the functional relations. This method is called fractional factorial design. In this study, the functional relations between the building heating/cooling loads and the building design factors were investigated using fractional factorial design. After the sets of trials to analyze the relation were prepared using the experimental design, the commercial dynamic building energy simulation program, TRNSYS [20], was used to estimate the heating and cool-

Table 3
The US climate zones and selected representative cities.

Climate Zone	City	Climate feature	Weather file in TRNSYS	References
1A	Miami	Hot, humid	US-FL-Miami-12839	[18]
2B	Phoenix	Hot, dry	US-AZ-Phoenix-23183	[19]
3C	San Francisco	Marine	US-CA-San-Francisco-23234	
4A	Baltimore	Mild, humid	US-MD-Baltimore-93721	
5A	Chicago	Cold, humid	US-IL-Chicago-94846	
6B	Helena	Cold, dry	US-MT-Helena-24144	
7	Duluth	Very cold, dry	US-MN-Duluth-14913	
8	Fairbanks	Extremely cold, dry	US-AK-Fairbanks-26411	

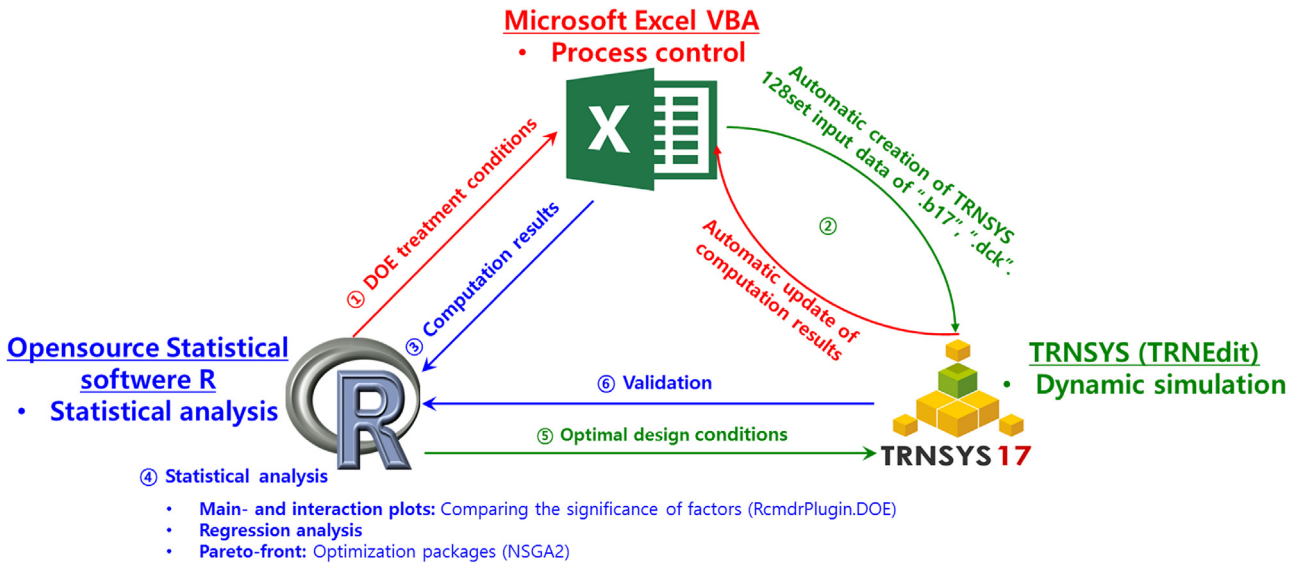

Fig. 2. Workflow of the automated analysis.

ing loads of the buildings having the selected design factors. The functional relation between the building heating/cooling loads and building design factors was analyzed, and the polynomial form of the relations shown in Eq. (1) was obtained using the DOE package of the open-source statistics software package R [21,22].

$$Y = c_0 + \sum_{i=1}^{N} c_i X_i + \sum_{j=1,k=j+1,}^{N} c_{jk} X_j X_k \quad (1)$$

In. Eq. (1), X and Y respectively represent the level (or value) of each design factor and the corresponding output value, various coefficients c's are coefficients of terms in the polynomial, and N is the number of design factors considered. The letters i, j, and k are dummy indexes. The second and third terms on the right side of Eq. (1) represent the main and second order interaction effects of the design factors upon the output. The impacts of the main and interaction effects upon the cooling and heating loads are discussed in Sections 3.1 and 3.2, respectively. Using the resultant polynomials, the optimum combinations of building design factors that yield the minimum building heating/cooling loads are searched for by adopting the multicriteria optimization algorithm provided by R, Non-dominated Sorting Genetic Algorithm II (NSGA-2) [23], for each climate zone. Section 3.3 discusses the optimization results in detail.

2.3. Experimental design

The workflow of the automated analysis process is outlined in Fig. 2. Once the treatments of DOE are determined considering the number of parameters and the resolution in R, the information is fed into Microsoft Excel [24], which controls the whole analysis process. Excel creates the input files using template sheets and automatically launches TRNSYS simulations using the files. The results are automatically accumulated in an Excel sheet, which provides raw data for R to perform statistical analysis such as regression and optimization, which provides the optimal design factor sets for minimizing the building energy loads. The results are elucidated and validated [15].

3. Results and discussion

3.1. Impacts of building design parameters upon building cooling load in different climate zones

Fig. 3 shows half-normal plots of the relative impacts of the main and interaction effects of building design factors upon cooling load in (a) Baltimore and (b) San Francisco. A half-normal plot is a graphical tool that uses these ordered estimated effects to help assess which factors are important and which are unimportant. To determine the ranked list of factors from a half-normal plot, simply scan the horizontal axis absolute effects [25]. Fig. 4 compares each factor's influence upon the cooling load in different climate zones using bar plots. The relative importance of the factors in different climate zones is compared using pie charts in Fig. 5, where the size of each slice represents the relative magnitude of the factor's impact on the cooling load in the given zone. The relative size of the pies represents the relative magnitude of cooling load in different cities.

It was found that SHGC, which directly affects the heat gain from insolation, was the most influential factor upon the building cooling load in (a) Baltimore and (b) San Francisco, as shown in Fig. 3. In Fig. 4, the bars for SHGC are taller than those for the other factors, leading to the same conclusion. The positive values for SHGC in the bar plot imply that the cooling load increases with increasing SHGC. Also, its impact decreases with decreasing climate zone number. The area-weighted solar irradiance sum of the building envelope for operating hours during the cooling season expressed in Eq. (2), was compared with the impacts of SHGC for different places in Fig. 4, and showed the same trend for the different cities.

$$\begin{bmatrix}\text{The area weighted average flux}\\ \text{of solar irradiation sum}\\ \text{for the operating hours}\\ \text{during the cooling season}\end{bmatrix}\left(Wh/m^2\right) = \text{area weighted average}\left[\sum_{\text{Cooling season}}\left(\sum_{\text{Operating hour}}\text{Solar irradiation flux}\right)\right] \quad (2)$$

The change in the effect of SHGC could be attributed to the differences in solar irradiance among the regions. However, the relative

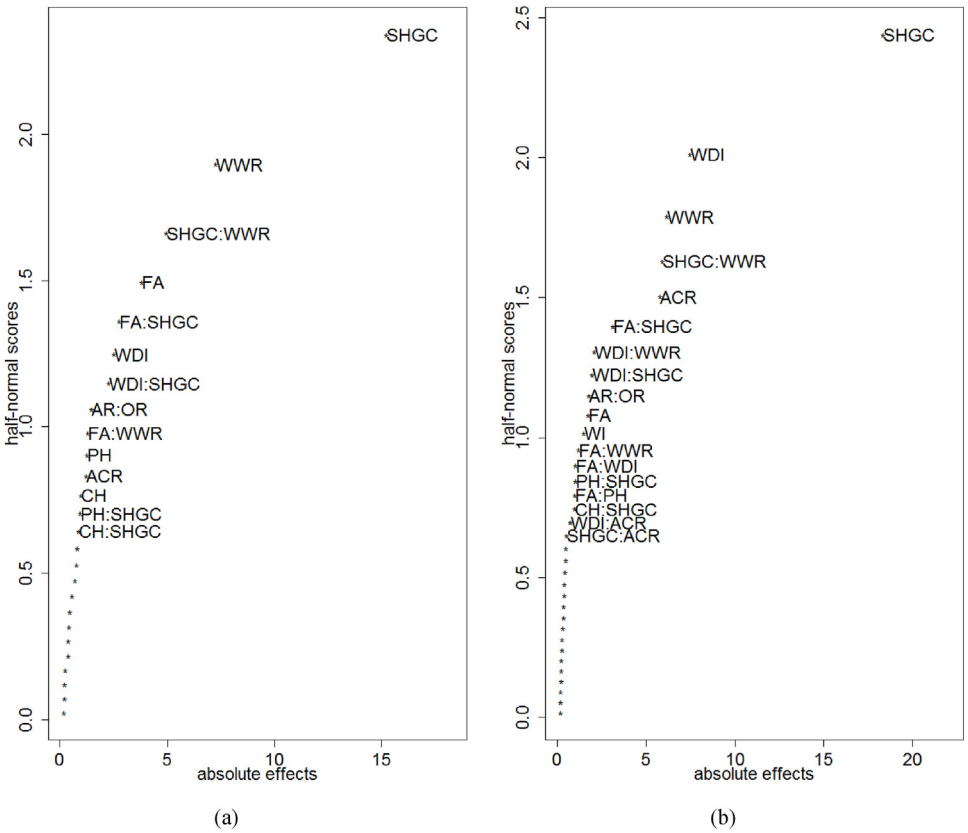

Fig. 3. Half-normal plots of the main and interaction effects of building envelope design factors for the cooling loads in (a) Baltimore and (b) San Francisco.

importance of SHGC was nearly constant for all climate zones, as shown in Fig. 5.

WWR was determined to be another important factor affecting the cooling load. It affects the building energy loads by affecting the area of solar irradiation and the area of the thermal transmission resistance of the building envelope. It is necessary to consider the combined impacts of SHGC and WDI to explain the impact of WWR because SHGC changes the solar irradiation and WDI alters the thermal transmission resistance of the glazing. WWR was the second most impactful factor in all zones except for San Francisco, as shown in Fig. 3. The interaction between SHGC and WWR was found to be another important effect, with positive magnitude; this interaction can be explained as an effect of WWR upon SHGC, whereby an increase in the glazing area (WWR) increases the SHGC. The impact of WWR upon cooling load was found to decrease generally with decreasing climate zone number, with an exception for San Francisco, as shown in Fig. 4, which could be explained by considering the impact of WDI simultaneously.

WDI followed WWR in main effect importance, except in San Francisco, where WDI was more influential than WWR (Figs. 3 and 4). WDI represents the heat transfer resistance of glazing, and during the cooling season, the temperature difference between the surroundings and the building set temperature acts as the driving force for heat transfer. The line in the WDI bar plot in Fig. 4 shows the product of the number of cooling months and the average temperature difference between the set and outdoor temperatures during operating hours in the cooling season for each zone, representing the total cooling load in terms of the temperature difference. The temperature difference is the greatest in San Francisco, and this explains the unusual behavior of WDI there. The average outdoor temperature is mostly lower than the set temperature, leading to negative values in the WDI bar plots in Fig. 4, so that upper levels of WDI, or lower thermal resistances, are better to lower the cooling load. It is expected that the impact would become more significant with WWR. Increasing WWR in San Francisco would increase the cooling load as a result of the interaction with SHGC while decreasing it together with WDI by enlarging the glazing surface for heat transfer, which explains the slight dip in the influence of WWR in San Francisco in the overall trend shown in Fig. 4. Phoenix was found to be the only place where the average outdoor temperature (28.5 °C) was higher than the building set temperature (26 °C) during the cooling season, and thus it was the only place for which WDI had a positive impact upon cooling load. WI represents the thermal transmission resistance through the wall, a resistance usually greater than that of the windows, WDI. Therefore, WI showed the same trends as WDI but with less impact, as shown in Fig. 4.

FA and its interactions with SHGC, WDI, and WWR were found to be other significant building design factors (Fig. 3). This implies that FA contributes to the cooling load by affecting the surface-to-volume ratio or the surface area of solar irradiation, and thus the heat transmission through the windows and the walls to the building, in a way similar to WWR. In Fig. 4, FA has negative values for all climate zones, meaning that increases in FA, which lower the portion of building perimeter area directly receiving solar irradiation, decrease the cooling load. The impact of FA generally decreases with climate zone number, with an exception from the general trend in San Francisco, where the effect of solar irradiation augmentation balances that of heat removal through glazing.

The same explanation holds for AR, CH, and PH, which have weaker impacts than FA as shown in Fig. 5. Increasing these values leads to increased glazing area to receive solar irradiation, and their effects are of opposite sign to FA as shown in Fig. 4.

ACR affected the cooling load basically in the same way as WDI (Fig. 4); infiltration produces heat gain or loss proportional to the temperature difference between the surrounding and set temper-

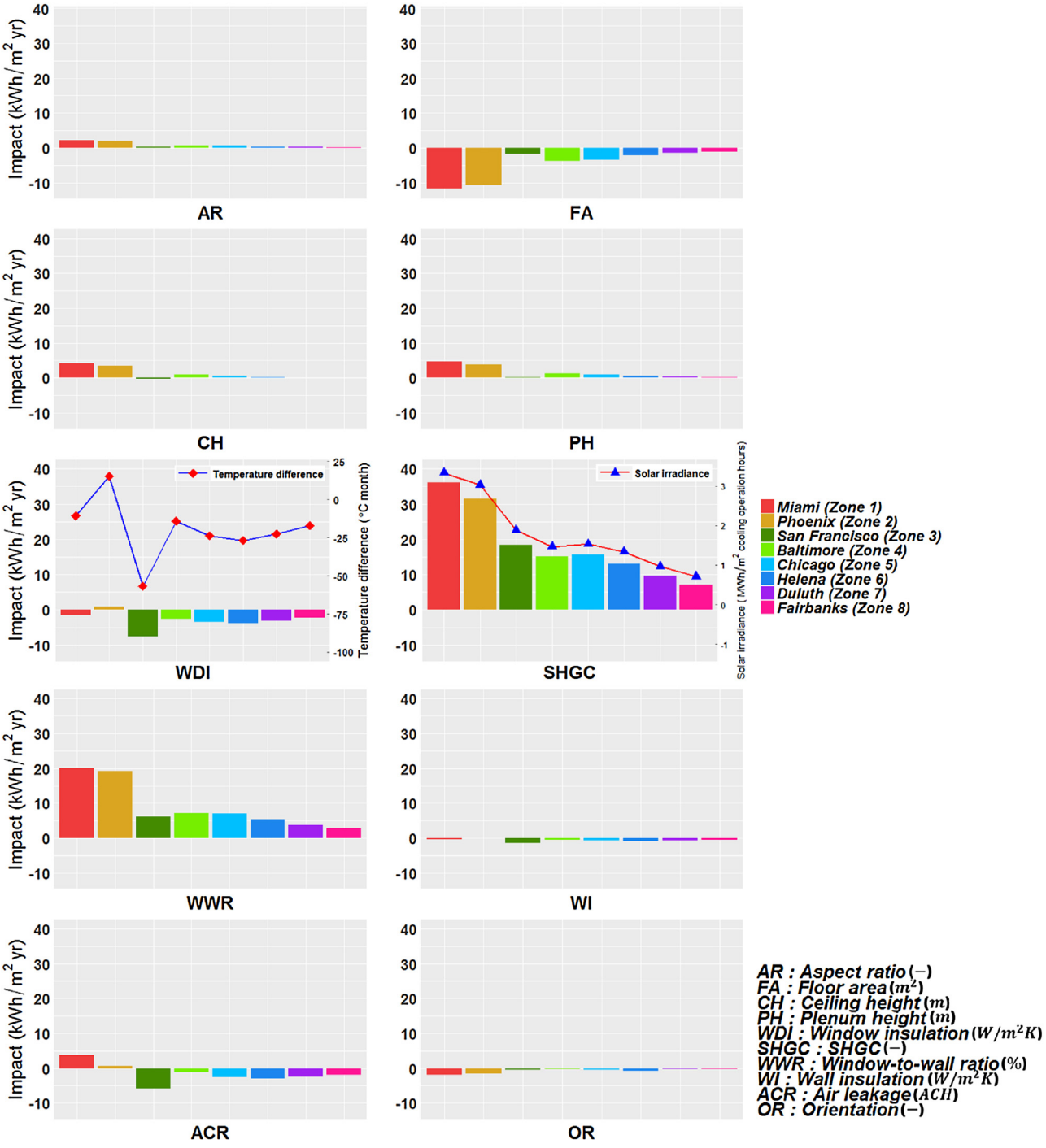

Fig. 4. Bar plots comparing the impact of each building envelope design factor upon the building cooling load in the eight cities considered.

atures. The difference originates from the latent heat needed to control relative humidity (RH) at the set point, 50%. If the RH of the surrounding air is higher than the set point, the latent heat to remove the corresponding absolute humidity (AH) adds to the cooling load. In the case of lower RH, it does not function as a cooling load. The latent heat due to higher RH and longer cooling season impose additional cooling load in Miami compared with the conditions in Phoenix, so the cooling load increase with increased ACR in Miami is greater than that in Phoenix, although the cooling load due to sensible heat in Phoenix outweighs that in Miami. Infiltration lowers the cooling load in other climate zones because the surrounding temperature is mostly lower than the set temperature. Due to the lower outdoor temperature and the longer cooling seasons in climate zones 3–8, the cooling load drop with increasing ACR was found to be the most significant in San Francisco.

The impact of OR was weakest among the factors considered, as shown in Fig. 5; west orientation was preferable to reduce cooling load.

Based on the above findings, the building envelope design factors considered in the current study were classified into three groups. Group 1 includes SHGC only, a factor that directly affects the heat gain from the solar irradiation. The same behaviors of the area weighted average flux of solar irradiation sum for the operating hours during the cooling season and the impact of SHGC on the

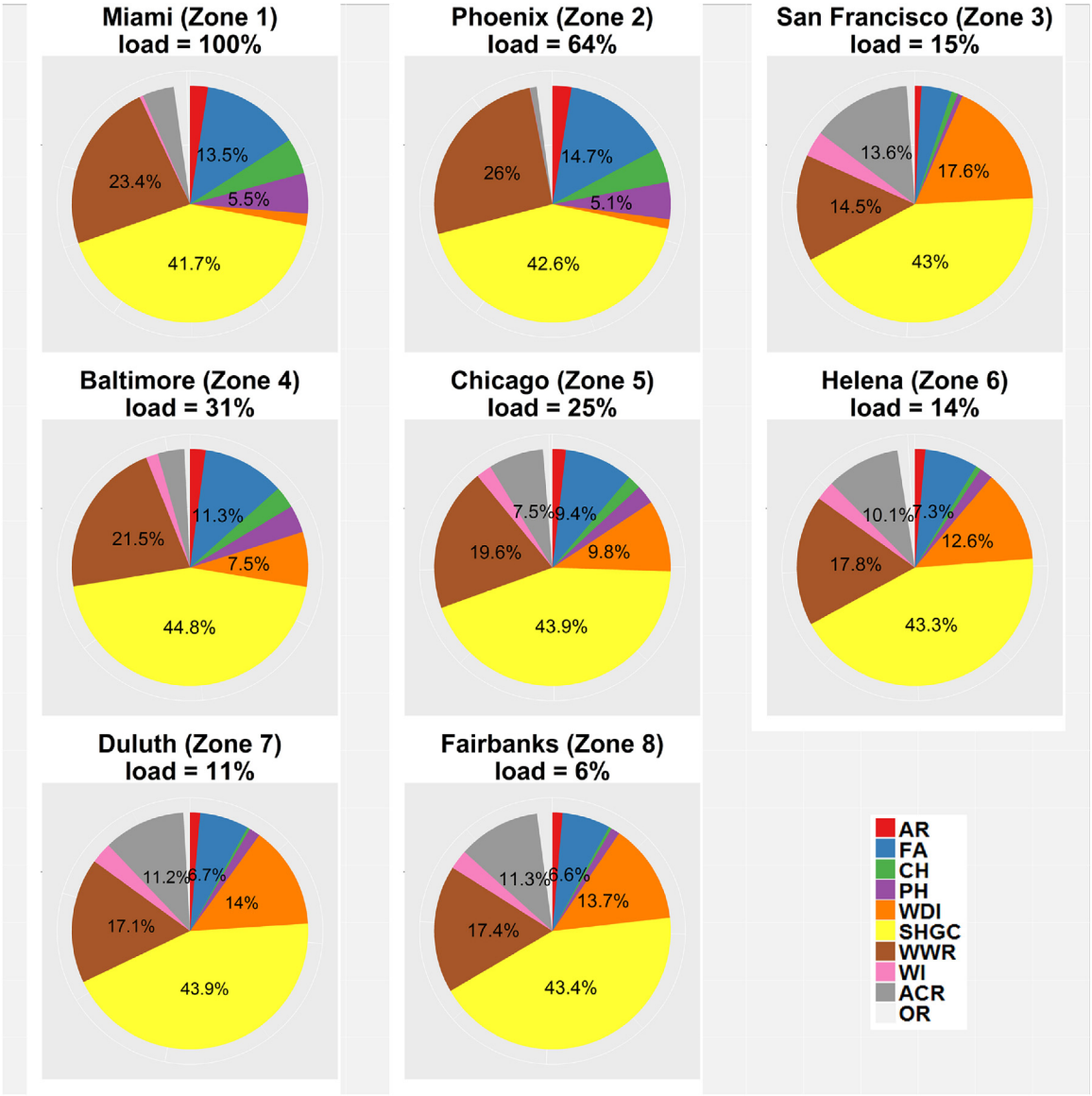

Fig. 5. Pie charts comparing the relative impact of building envelope design factors upon the cooling load in the eight cities considered.

cooling load in Fig. 4 supports the classification. Group 2 comprises WDI, WI, and ACR, factors whose impacts upon building energy load vary with the differences in temperature and RH between the set and outdoor conditions. The same trend in the variations of WDI, WI, and ACR with that of the product of the number of cooling months and the average temperature difference between the set and outdoor temperatures during operating hours in the cooling season in Fig. 4 verifies the classification. The slight difference in the behavior of ACR is due to the different impact of latent heat according to the climate zone. Group 3 comprises WWR, AR, FA, CH, and PH, factors that contribute to the energy load by changing the effective area for solar irradiation and heat conduction through the building envelope.

3.2. *Impacts of building design parameters on building heating load in different climate zones*

Fig. 6 shows half-normal plots of the building heating load in (a) Baltimore and (b) San Francisco. Figs. 7 and 8 show the absolute and relative impacts of each building design factor upon the heating load, respectively. Note that there is no heating load in Miami.

WDI, ACR, SHGC, and WWR were the key factors that most affected the heating load, as shown in Fig. 6. As discussed in the previous section, ACR and WDI affect the building energy loads by means of the same mechanism; the temperature difference between the set and surrounding temperatures is the impetus for building heat loss, leading to the same trends of the bar plots for these factors in Fig. 7. The impacts of ACR and WDI increased with increasing climate zone number because this corresponds to increasing temperature differences and number of months in the heating season. The line in the WDI bar plot shows the product of the number of heating months and the average temperature difference between the set and outdoor temperatures during operating hours during the heating season for each zone. The role of WI is the same as that of WDI, but WI has a lower impact due to the larger thermal transmission resistance of walls compared with that of windows. Increasing SHGC increases the heat gain from solar irradiation, thereby lowering the heating load. The impact of SHGC was found to sync with the solar irradiation amount, as can be seen by comparing the SHGC bar graph and the corresponding line in Fig. 7, both of which peak for Duluth. The trend of WWR impacts resembles that of WDI because WWR alters the effective glazing

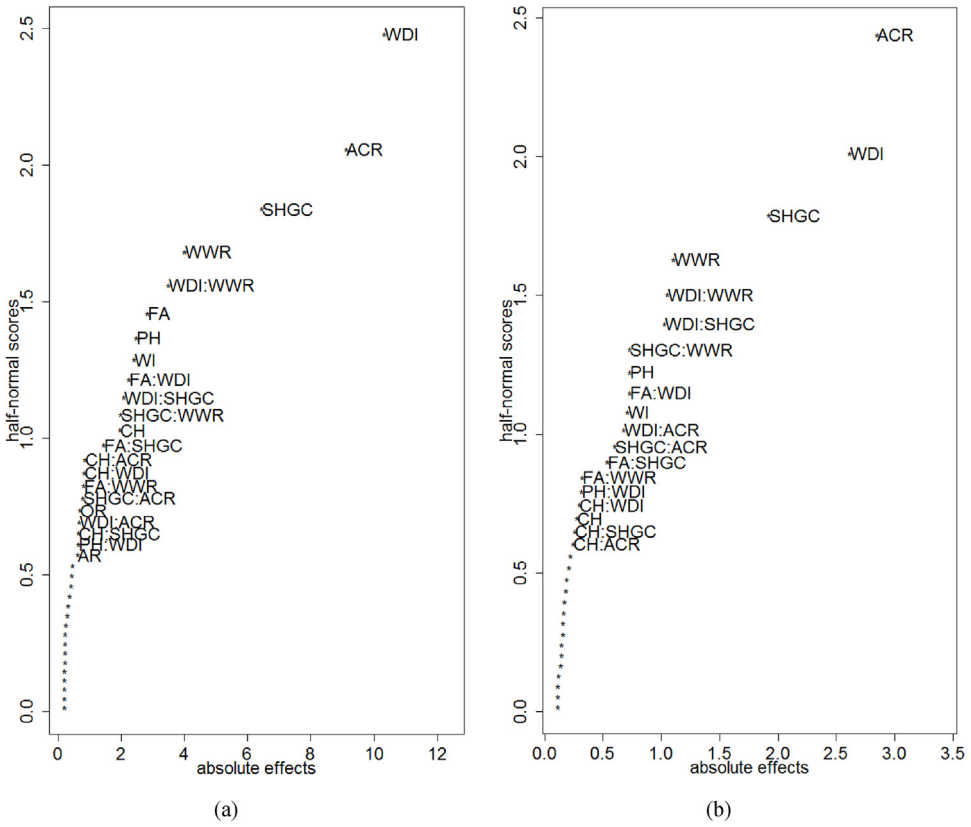

Fig. 6. Half-normal plots of the main and interaction effects of building envelope design factors for the heating loads in (a) Baltimore and (b) San Francisco.

surface area and thus the heat loss. However, its impact in Duluth was weaker than that for WDI, which could be attributed to the fact that the solar irradiation is maximized there, balancing the heat gain from solar irradiation and the heat loss through windows.

The surface-to-volume ratio of the office decreases with increasing FA, thereby lowering the heating load, as shown in Fig. 7. The temperature difference during the heating season between the set and outdoor temperatures increases with the climate zone number; hence the impact of FA also increases with it. For the same reasons discussed above regarding the cooling load, AR, CH, and PH affect the heating load in the same manner as FA, but with the opposite sign compared to their effects upon the cooling load.

The impact of OR was weaker than the other factors, as shown in Fig. 7. In contrast to the case of cooling load, South facing lowers the heating load.

The same classification of building envelope design factors made above for the cooling load could be used to explain their impacts upon the heating load.

Table 4
Coefficients of the regression formula for cooling and heating loads in Baltimore (Eq. (1)).

Cooling load				Heating load			
Factor	Coefficient	Factor	Coefficient	Factor	Coefficient	Factor	Coefficient
Intercept	5.598×10^{1}	AR:SHGC	1.771	Intercept	-1.071×10^{1}	FA:CH	-1.247×10^{-3}
AR	−5.129	AR:WWR	1.456×10^{-2}	AR	2.521×10^{-1}	FA:PH	-1.205×10^{-3}
FA	1.094×10^{-2}	AR:OR	2.995	FA	7.031×10^{-3}	FA:WDI	-2.160×10^{-3}
CH	−2.546	FA:CH	-9.666×10^{-4}	CH	4.543×10^{-1}	FA:SHGC	5.807×10^{-3}
PH	2.174	FA:PH	-4.111×10^{-3}	PH	2.6	FA:WWR	-6.115×10^{-5}
WDI	−2.922	FA:WDI	3.807×10^{-4}	WDI	−2.177	FA:WI	-4.498×10^{-3}
SHGC	-2.071×10^{1}	FA:SHGC	-1.106×10^{-2}	SHGC	1.969×10^{1}	CH:WDI	1.602
WWR	-1.489×10^{-1}	FA:WWR	-9.866×10^{-5}	WWR	1.027×10^{-2}	CH:SHGC	−5.166
WI	−2.703	CH:SHGC	7.275	WI	2.071×10^{1}	CH:WWR	3.439×10^{-2}
ACR	−8.234	CH:WWR	7.159×10^{-2}	ACR	−6.747	CH:ACR	1.740×10^{1}
OR	−4.758	PH:SHGC	9.558	OR	-3.051×10^{-1}	PH:WDI	1.539
PH:WWR	7.457×10^{-2}	WDI:WWR	-2.813×10^{-2}	AR:FA	-4.024×10^{-4}	PH:SHGC	−3.629
WDI:SHGC	4.413	WDI:ACR	1.149	AR:WDI	4.177×10^{-1}	PH:WWR	3.841×10^{-2}
SHGC:WWR	7.366×10^{1}			AR:SHGC	-8.245×10^{-1}	PH:WI	5.053
				AR:WWR	1.538×10^{-2}	PH:ACR	7.575
				WDI:SHGC	−4.009	SHGC:WI	−4.312
				WDI:WWR	1.240×10^{-1}	SHGC:ACR	-1.579×10^{1}
				WDI:ACR	3.274	WWR:WI	-1.455×10^{-1}
				WDI:OR	2.195×10^{-1}	WWR:OR	1.595×10^{-2}
				SHGC:WWR	-2.933×10^{-1}		

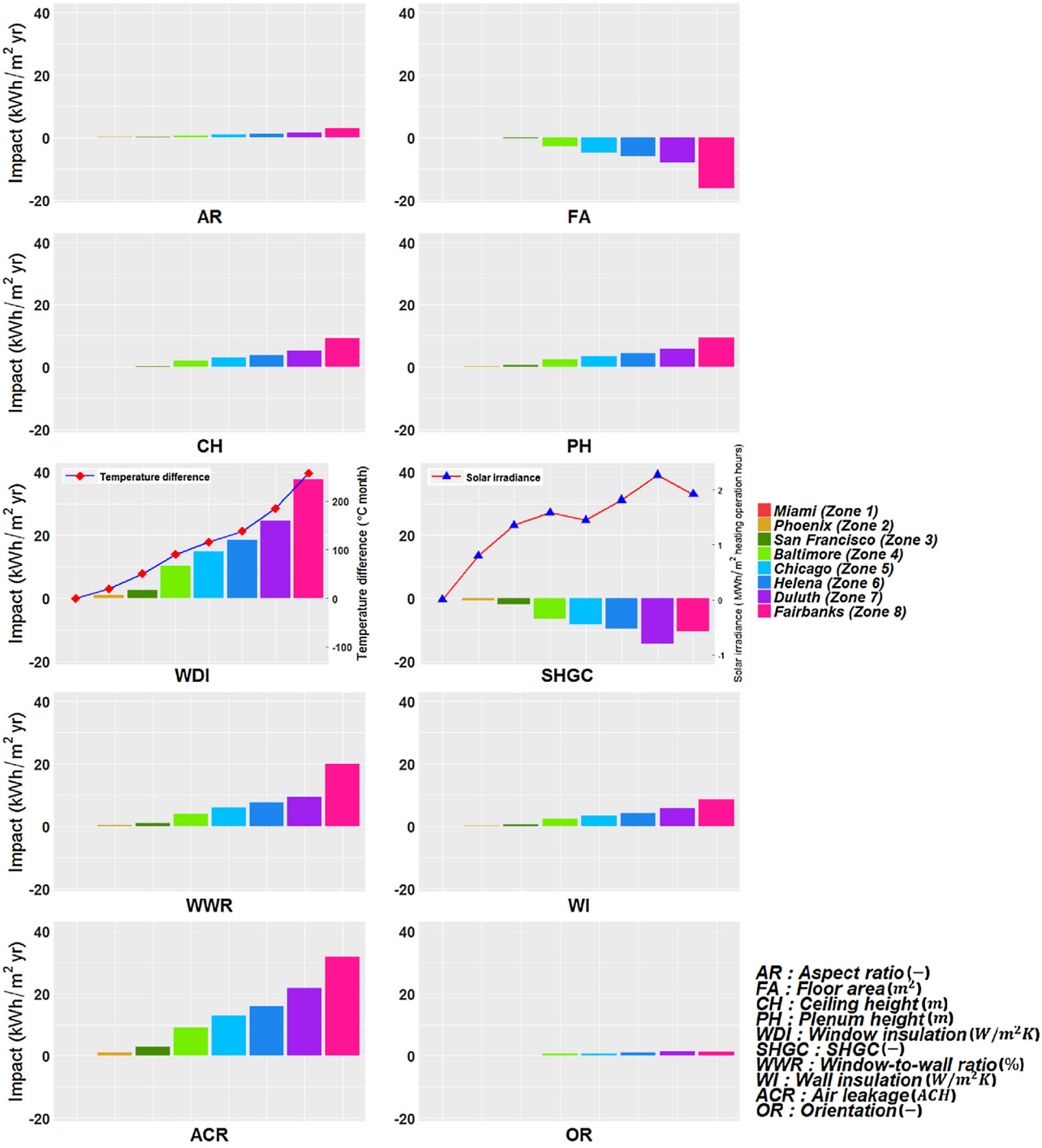

Fig. 7. Bar plots comparing the impact of each building envelope design factor upon the building heating load in the eight cities considered.

3.3. *Pareto fronts to minimize building energy loads in different climate conditions*

Fig. 9a–d show the cooling and heating loads of building design sets determined by using the regression formula in Eq. (1) for the cooling and heating loads in Baltimore (zone 4) and San Francisco (zone 3). As an example, Table 4 lists the coefficients of the regression formula for Baltimore. Fig. 9a–d show the TRNSYS simulation results and the predictions of the fitting formula for the two example cities. The coefficients of determination were 0.994 for the cooling load and 0.993 for the heating load of Baltimore, and 0.996 for the cooling load and 0.970 for the heating load of San Francisco. For the other cities, the coefficients of determination were all above 0.96; Table 5 summarizes the results. In Figs. 10 and 11, each circular symbol in the graphs represents a pair of cooling and heating loads calculated for a building design test set using TRNSYS simulation. The Pareto front is the curve in each graph connecting the points at which the magnitude of a load is minimized for a given magnitude of the other load; each curve was determined by a minimization process using the regression formula. The dashed lines represent 95% confidence intervals of the Pareto fronts.

Moving along a Pareto front from left to right, the cooling load decreases while heating load increases. In Figs. 10 and 11, the diamond points labeled with letters are the inflection points of the

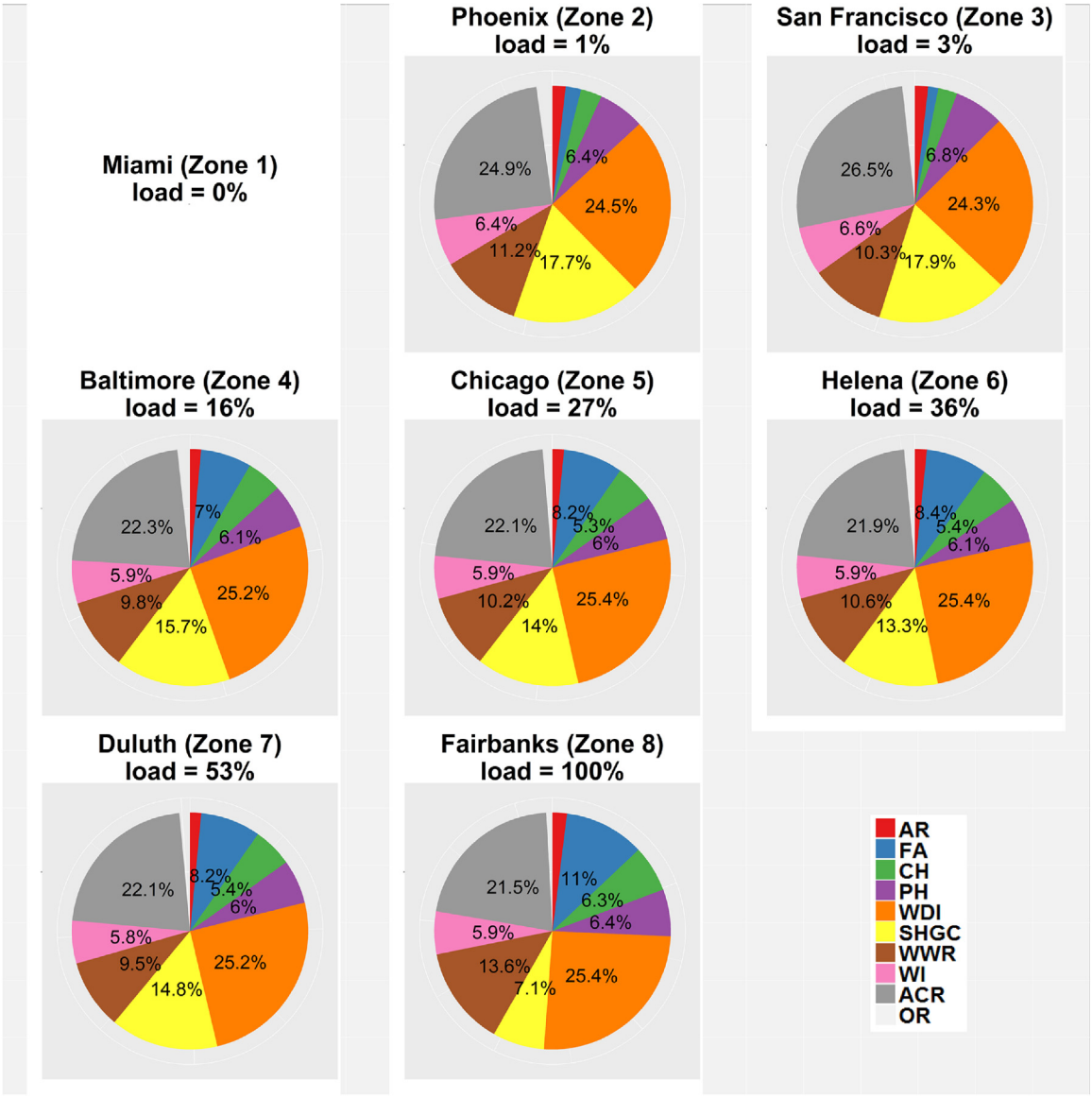

Fig. 8. Pie charts comparing the relative impact of building envelope design factors upon the heating load in the eight cities considered.

Table 5
Determination coefficients of the regression formula for cooling and heating loads in the cities considered.

Location	Cooling load	Heating load
Miami	0.9950	–
Phoenix	0.9945	0.9636
San Francisco	0.9958	0.9697
Baltimore	0.9944	0.9931
Chicago	0.9948	0.9955
Helena	0.9953	0.9959
Duluth	0.9952	0.9963
Fairbanks	0.9965	0.9981

Pareto fronts. Table 6 lists the levels of the factors corresponding to the inflection points for Baltimore. The levels of the factors vary between the connecting points, leading to changes in the cooling and heating loads. AR, PH, WWR and OR are fixed along the curve.

The levels of CH and SHGC decrease between points A and B in Fig. 10, decreasing the cooling load steeply while causing a relatively small increase in the heating load. FA, WDI, and WI change along the curve between points B and D, where the increase in heating load becomes steeper for a given amount of cooling load reduction. The levels of WI and ACR change between points D and E, where the heating load rise is very large with little reduction of the cooling load. The points on the Pareto front could be consid-

Table 6
Variation of the optimal selection sets of building envelope design factors along the Pareto curve for Baltimore.

Points	AR	FA	CH	PH	WDI	SHGC	WWR	WI	ACR	OR
A	1	1000	2.89	0.8	0.75	0.7	25	0.15	0.1	2
B	1	1000	2.4	0.8	0.75	0.2	25	0.15	0.1	2
C	1	1870	2.4	0.8	2.81	0.2	25	0.15	0.1	2
D	1	1000	2.4	0.8	2.84	0.2	25	0.19	0.1	2
E	1	1000	2.4	0.8	2.84	0.2	25	0.36	0.3	2

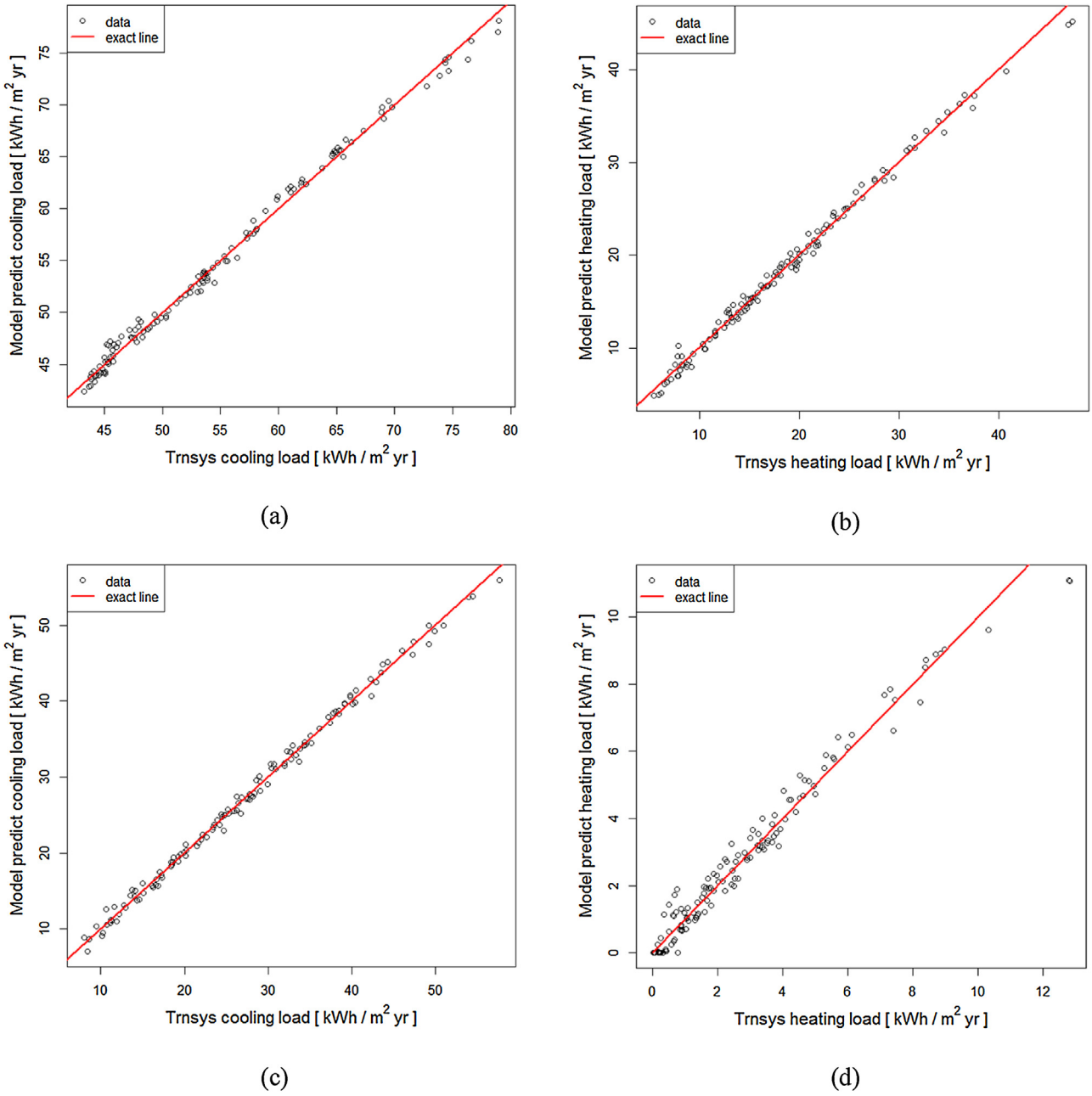

Fig. 9. Comparison of the results from TRNSYS simulations and regression formula for (a) cooling and (b) heating loads in Baltimore; and for (c) cooling and (d) heating loads in San Francisco.

ered as candidate designs for the building envelope to lower energy consumption.

Fig. 12a and b compare the coefficients of the main and interaction terms in the regression formula for the cooling and heating loads. Because the levels of the factors are normalized, the magnitudes of the coefficients represent the impacts of the main and interaction effects of the building design factors. For both loads, the signs of the coefficients were the same for AR, FA, CH, PH, and WWR, and they were believed to remain unaltered along the Pareto front at a glance. SHGC was found to be the most influential factor, and it had opposite signs for the cooling and heating loads, with a much greater magnitude of the cooling load. As SHGC decreases between the points A and B, the cooling load decreases rapidly, while the heating load increases mildly. Although CH should not change along the Pareto front, it was found to vary between points A and B due to its interaction with SHGC. This interaction arises as an effect of CH upon SHGC: increasing CH increases SHGC by increasing the surface subject to solar irradiation. In the section of the front between points B and D, WDI, which has different impacts on the cooling and heating loads, is the most influential factor. As WDI increases, the heating load increase exceeds the cooling load reduction. Although the main effect of increasing FA is to increase both the loads, its interaction with SHGC and WDI contributes to the change of the Pareto front in this section. ACR is another key factor that has a relatively small negative impact on the cooling load and a much greater positive impact on the heating load. Increasing ACR increases the heating load measurably while decreasing the cooling load negligibly between points D and E. WI contributes in the same manner as WDI but changes along the Pareto front in the region between C and E.

Fig. 11 and Table 7 show another example in San Francisco, where the building energy loads are lower than in the other cities

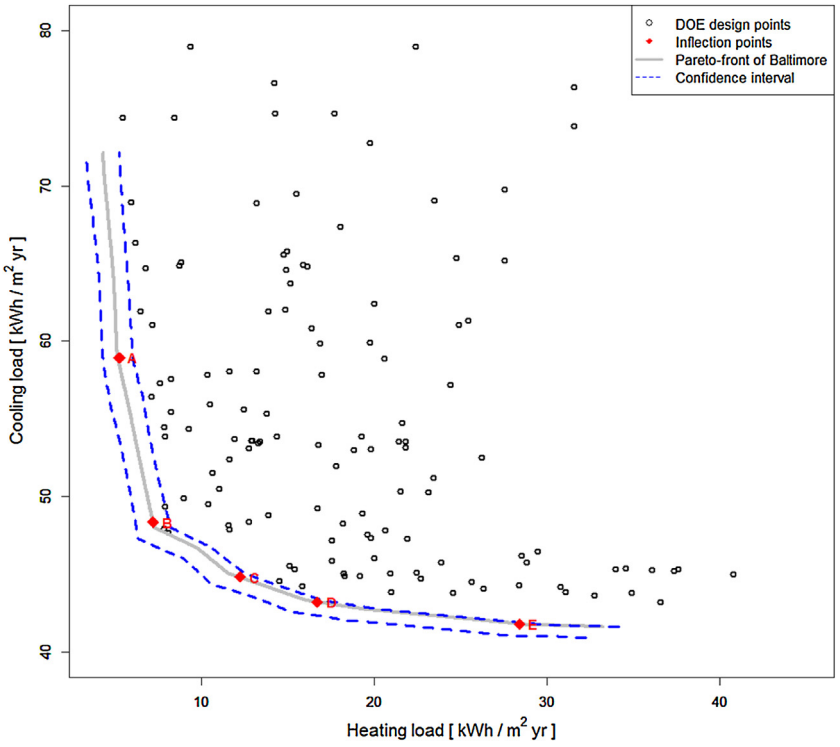

Fig. 10. The pareto-front curve of cooling and heating loads in Baltimore.

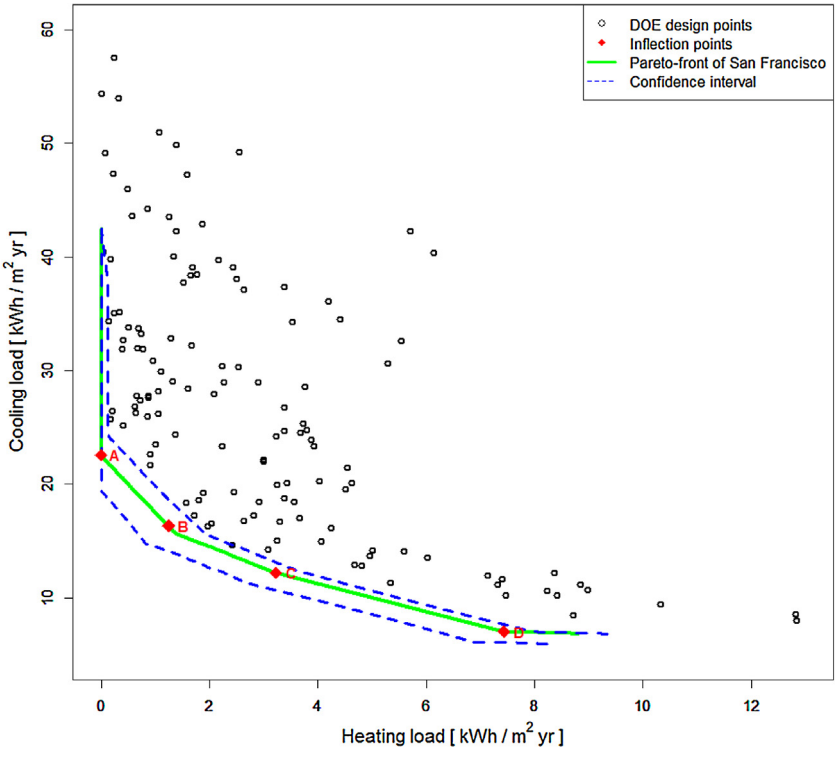

Fig. 11. The pareto-front curve of cooling and heating loads in San Francisco.

Table 7
Variation of the optimal selection sets of building envelope design factors along the Pareto curve for San Francisco.

Points	AR	FA	CH	PH	WDI	SHGC	WWR	WI	ACR	OR
A	1	1000	2.4	0.8	1.23	0.2	25	0.15	0.1	2
B	1	1039	2.4	0.8	2.72	0.2	25	0.15	0.1	2
C	2	1000	2.9	0.8	2.84	0.2	25	0.36	0.1	1
D	2	1000	2.9	0.8	2.84	0.2	25	0.36	0.3	1

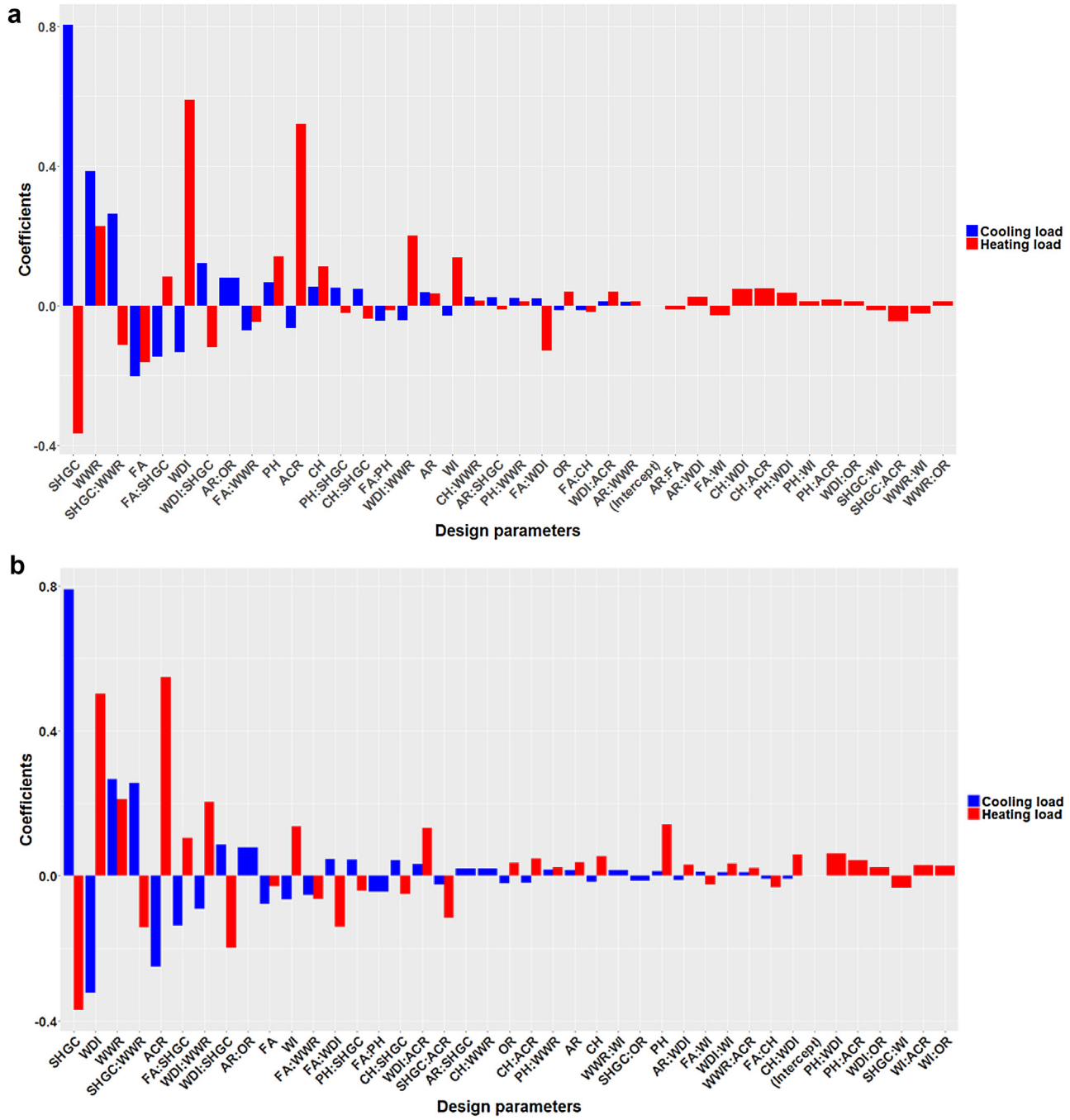

Fig. 12. (a) Comparison of regression coefficients of design factors in (a) Baltimore. (b) Comparison of regression coefficients of design factors in (b) San Francisco.

considered due to the cooler summer and warmer winter seasons. Depending on the set of building envelope design factors chosen, the office could be free of any heating load. There is no reason to choose any point above point A along the y-axis, where SHGC decreases. Between points A and B, WDI increases, indicating that reducing window thermal insulation to reduce cooling load comes at the cost of increasing the heating load. Along the segment between points B and C, CH and WI increase, enhancing heat rejection through the envelope during the cooling season but also yielding a heating load increase. ACR further reduces the cooling load and increases the heating load between points C and D for the same reason. Fig. 12b compares the sign and magnitude of each term in Eq. (1) for the cooling and heating loads in San Francisco. SHGC is the most significant factor, with opposite signs for the cooling and heating loads, and it plays a role in the segment above point A. WDI is the factor with the next greatest impact on the Pareto front line as discussed previously. Although WWR is another important factor, it does not appear to vary along the Pareto front line, because it has the same signs for both cooling and heating loads. The Pareto front curves in other cities could be explained in the same manner.

Fig. 13 compares the Pareto fronts for cities in different climate zones. Miami has only cooling load, so the point with the maximum WDI and WI and the minimum level of the other factors, and with east facing, should be the optimum building envelope to save energy. San Francisco was found to have the lowest building energy loads. With increasing climate zone number, the Pareto front shifts to the lower right of the graph of cooling vs. heating load, yield-

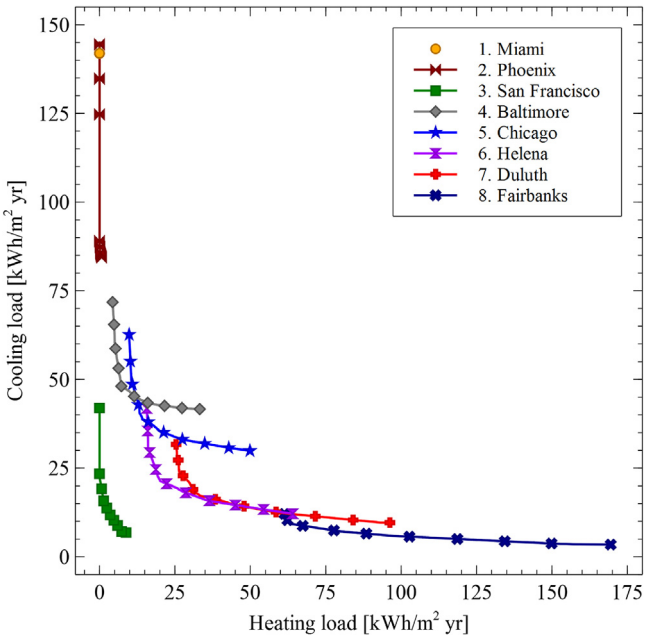

Fig. 13. Comparison of Pareto-front curves in the eight cities considered.

ing elongated segments of large heating load increase with small corresponding reductions in cooling load.

4. Conclusions

The complex dependence of building energy loads upon building envelope design factors and weather conditions was explicitly analyzed using an experimental design. The best sets of design factor selections for load reduction were determined for each climate zone by using an optimization package of the statistical analysis package R. The most important conclusions drawn from the current research are summarized as follows.

- Weather conditions including dry-bulb temperature, RH, AH, and insolation are found to contribute to the building energy loads in a coupled manner with the building envelope design factors, and their individual effects and causes were well analyzed by using the experimental design technique.
- The considered building envelope design factors could be classified into three groups. SHGC is the only member of group 1, which directly controls the solar irradiation into the building. Group 2 includes WDI, WI, and ACR, whose impacts depend on the temperature difference between the building's set and outdoor temperatures. Group 3 includes WWR, AR, FA, CH, and PH, which affect the building energy loads by varying the effective building area for the solar irradiation and the heat conduction through the walls and windows.
- Among the ten building envelope parameters considered in this study for the buildings of given layout under the 8 US climate conditions, the impacts of SHGC and WWR on the building cooling load were found to be the most influential ones forming 43 and 20% shares on average respectively. WDI, ACR, SHGC, and WWR were observed to be the significant parameters affecting the heating load, with which 25, 23, 14, and 11% of the load variation with the design alteration could be explained.
- San Francisco showed unique cooling load behavior due to the low outdoor temperature during the cooling season. The larger temperature difference between the set and outdoor temperature enhances heat dissipation through the windows and walls, making San Francisco an exception in the overall trend of the impact of WDI in lowering the cooling load. In San Francisco, the promotion of heat dissipation with increasing WWR balances with the solar irradiation through the windows to undermine the impact of WWR there.
- In Pareto fronts representing candidate point sets of building envelope design factors to minimize the building energy use, opposite impacts of the main effect of a factor and of the interaction effect of couples of two factors in a segment of a Pareto front as well as the specific range of each design factor were found to be the causes of the observed inflection points. The interaction between factors also attributed to the behavior of the Pareto fronts.

References

[1] U.S. Department of Energy, Zero Energy Build. (2017) http://energy.gov/articles/energy-department-invests-19-million-improve-efficiency-nation-s-buildings.
[2] J. Cho, J. Kim, S. Lee, J. Koo, A bi-directional systematic design approach to energy optimization for energy-efficient buildings, Energy Build. 120 (2016) 135–144.
[3] L.G. Caldas, L.K. Norford, A design optimization tool based on a genetic algorithm, Autom. Constr. 11 (17) (2002) 3–184.
[4] J.A. Wright, H.A. Loosemore, R. Farmani, Optimization of building thermal design and control by multi-criterion genetic algorithm, Energy Build. 34 (2002) 959–972.
[5] M. Wetter, J. Wright, A comparison of deterministic and probabilistic optimization algorithms for nonsmooth simulation-based optimization, Build. Environ. 39 (2004) 989–999.
[6] L. Yang, J.C. Lam, C.L. Tsang, Energy performance of building envelopes in different climate zones in China, Appl. Energy 85 (2008) 800–817.
[7] I. Jaffal, I. Christian, G. Christian, Fast method to predict building heating demand based on the design of experiments, Energy Build. 41 (2009) 669–677.
[8] L. Magnier, F. Haghighat, Multiobjective optimization of building design using TRNSYS simulations genetic algorithm, and artificial neural network, Build. Environ. 45 (2010) 739–746.
[9] X. Gong, Y. Akashi, D. Sumiyoshi, Optimization of passive design measures for residential buildings in different Chinese areas, Build. Environ. 58 (2012) 46–57.
[10] V. Machairas, A. Tsangrassoulis, K. Axarli, Algorithms for optimization of building design: a review, Renew. Sustain. Energy Rev. 31 (2014) 101–112.
[11] A. Nguyen, S. Reiter, P. Rigo, A review on simulation-based optimization methods applied to building performance analysis, Appl. Energy 113 (2014) 1043–1058.
[12] J. Schnieders, W. Feist, L. Rongen, Passive Houses for different climate zones, Energy Build. 105 (2015) 71–87.
[13] N. Delgarm, B. Sajadi, S. Delgarm, F. Kowsary, A novel approach for the simulation-based optimization of the buildings energy consumption using NSGA-II: case study in Iran, Energy Build. 127 (2016) 552–560.
[14] F. Goia, Search for the optimal window-to-wall ratio in office buildings in different European climates and the implications on total energy saving potential, Sol. Energy 132 (2016) 467–492.
[15] Jun Xu, Jin-Ho Kim, Hiki Hong, Junemo Koo, A systematic approach for energy efficient building design factors optimization, Energy Build. 89 (2015) 87–96.
[16] ANSI/ASHRAE Standard 62-2007, Ventilation for Acceptable Indoor Air Quality, 2007.
[17] Ministry of Land, Transport and Maritime Affairs, Guideline of Window System Design for Building Energy Saving, Ministry of Land, Transport and Maritime Affairs, 2012 (in Korean).
[18] NREL, U.S. Department of Energy Commercial Reference Building Models of the National Building Stock, NREL, 2011.
[19] Advanced Energy Design Guide for Small to Medium Office Buildings, ASHRAE Inc., 2011.
[20] S.A. Klein, TRNSYS 17-A Transient System Simulation Program, Solar Energy Laboratory, University of Wisconsin, Madison, 2010 http://sel.me.wisc.edu/trnsys.
[21] R Core Team, R: A Language and Environment for Statistical Computing, R Foundation for Statistical Computing, Vienna, Austria, 2014 http://www.R-project.org/.
[22] U. Groemping, RcmdrPlugin. DoE: R Commander Plugin for (industrial) Design of Experiments, R package version 0, 2014, pp. 12–13 https://CRAN.R-project.org/package=RcmdrPlugin.DoE.
[23] C.-S. Tsou, nsga2R: Elitist Non-dominated Sorting Genetic Algorithm based on R, R package version 1.0, 2013 https://CRAN.R-project.org/package=nsga2R.
[24] Microsoft, Microsoft Excel: computer software, Redmond, Washington, 2016 https://products.office.com/en-us/excel.
[25] NIST/SEMATECH, e-Handbook of Statistical Methods, 2013 http://www.itl.nist.gov/div898/handbook/,date.

[26] Ministry of Land, Transport and Maritime Affairs, Guideline of Window System Design for Building Energy Saving, Ministry of Land, Transport and Maritime Affairs, 2012 (in Korean).
[27] ASHRAE, Standard-Energy Standard for Buildings Except Low-Rise Residential Buildings, ASHRAE Inc., Atlanta, 2007.
[28] PNNL, U.S. Department of Energy Infiltration Modeling Guidelines for Commercial Building Energy Analysis, PNNL, 2009.
[29] Ministry of Land, Transport and Maritime Affairs, Design Guideline for the Energy Saving of Public Buildings in Innovation City, Ministry off Land, Transport and Maritime Affairs 2010 (in Korean).
[30] Korea Energy Management Corporation, Explanation of Energy Saving Design Standard in Buildings in Innovation City, Korea Energy Management Corporation, 2011 (in Korea).
[31] ANSI/ASHRAE Standard 55-2010, Thermal Environmental Conditions for Human Occupancy, 2010.
[32] ANSI/ASHRAE Standard 62-2007,V entilation for Acceptable Indoor Air Quality, 2007.
[33] ANSI/ASHRAE Standard 55-2010, Thermal Environmental Conditions for Human Occupancy, 2010.